A silver complex of hyaluronan-lipoate (SHLS12): synthesis, characterization and biological properties

Pasquale Sacco[1], Alessandra Sechi[2], Antonia Trevisan[2], Fabrizio Picotti[2], Rita Gianni[2], Luca Stucchi[2], Matteo Fabbian[2], Marco Bosco[2], Sergio Paoletti[1], and Eleonora Marsich[3*]

[1]Department of Life Sciences, University of Trieste, Via Licio Giorgieri 5, I-34127 Trieste, Italy

[2]SIGEA Srl, AREA Science Park, loc. Padriciano 99, I-34149 Trieste, Italy

[3]Department of Medical, Surgical and Health Sciences, University of Trieste, Piazza dell'Ospitale 1, I-34129 Trieste, Italy

***Corresponding author**

Email: emarsich@units.it

Phone: +39-040-5588733

Abstract

In this study we present a novel silver complex of hyaluronan-lipoate (SHLS12) in a gel-state form. NMR analysis, conductometry and elemental analysis demonstrated stable non-covalent interactions between silver ions and the polysaccharide-lipoate backbone, whereas rheological investigations confirmed its gel-like physical-chemical behavior. Biological studies showed the ability of SHLS12 to exert a straightforward activity against different bacterial strains grown in sessile/planktonic state. The biocompatibility was also proved towards two eukaryotic cell lines. By considering both its ability to preserve antibacterial properties when exposed to the serum protein BSA and its low susceptibility to be degraded by hyaluronidase enzyme, this novel complex may be considered as a promising biomaterial for future *in vivo* applications.

Keywords: Hyaluronan, hyaluronan-lipoate, silver complex, gel, bacteria barrier effect.

1. Introduction

The extended use of silver and silver-derivatives has since long time gained appeal because of their ability to exert antibacterial activity towards a wide number of bacteria strains. This surely represents an undeniable advantage for the healthcare worldwide, considering the evolution of microorganisms, in particular their resistance against multiple antibiotics.(Klasen, 2000) With the advancement of nanotechnology, nano-crystalline forms of silver metal can be easily obtained by exploiting reliable protocols so as to tune their dimension and shape.(Gunasekaran, Nigusse, & Dhanaraju, 2011) Nevertheless, it is a hitherto diffuse opinion considering silver ions (Ag^+) as responsible for the antimicrobial activity.(Knetsch & Koole, 2011) Indeed, the work of Xiu *et al.* gave an excellent contribution to clarify this question, inferring that Ag^+ is the definitive molecular toxicant.(Xiu, Zhang, Puppala, Colvin, & Alvarez, 2012) In this scenario, Ag^+ ions formed by oxidation of the (reduced) metal core form a silver ion corona surrounding silver nanoparticles; physical contact of bacteria with such Ag^+ ions, dissolved and released in the environment surrounding the nanoparticles, is at the root of their toxicity towards prokaryotic cells. As a consequence, the development of innovative biomolecules to capable of firmly coordinating silver ions in a non-toxic form for the eukaryotic cells and so exploitable in biomedical products is a key challenge.

A noteworthy candidate to this purpose is hyaluronan (HA). HA is a polysaccharide naturally present in the human body and it is composed of the regularly alternating repeat of β (1→4) linked **D**-glucuronic acid and β (1→3) linked **D**-N-acetylglucosamine. It is widely considered a very interesting biopolymer because of its peculiar physical, chemical and biological properties.(Collins & Birkinshaw, 2013) There are very few studies concerning the ability of HA to foster the binding and stabilization of silver in different chemical forms compared to other biopolymers, *e.g.* chitosan or alginate.(S. J. Lee et al., 2014), (Yang, Zheng, Han, Jiang, & Chen, 2015) For example, Abdel-Mohsen *et al.* fabricated HA fibers *via* wet-spinning technique, which were able to form and to

stabilize silver nanoparticles.(Abdel-Mohsen et al., 2012) Chudobova *et al.* demonstrated the formation of hyaluronate-silver complexes after the addition of silver nitrate to a solution of HA.(Chudobova et al., 2013)

The basic idea for the present work is to exploit a hyaluronan-lipoate derivative (known as Lipohyal)(Picotti et al., 2013) to obtain a stable hyaluronan-silver complex. Lipohyal (Figure S1 of the Supplementary Material) is a mixed ester of lipoic and formic acids of hyaluronan which was demonstrated to possess radical scavenging properties, high resistance *versus* enzymatic degradation by hyaluronidase and the possibility to be cross-linked by means of UV irradiation in order to obtain a stable hydrogel with peculiar viscoelastic properties.(Picotti et al., 2013)

Lipoate is a disulphide derivative of octanoic acid and it has been well known to be a powerful tool for the treatment and prevention of many pathologies involving a defect of the oxidative-reductive cellular pathway.(Bustamante, 1998),(Kagan et al., 1992) Ramachandran *et al.* developed a lipoate-silver nanoparticles complex to be used as an adjuvant in cancer radiotherapy and also to enhance the anti-tumor activity of gamma radiation, but antibacterial studies were not reported.(Ramachandran & Krishnan Krishnan Nai, 2011)

In the present paper we present a novel silver complex of sodium hyaluronate-lipoate (SHLS12) capable to coordinate silver ions. SHLS12 is produced by introducing slight modifications in the synthetic pathway of Lipohyal, mainly devoted to avoid the presence of formate ester residues linked on the polymeric chain. This compound is shown to advantageous provide the combination of distinctive and novel physical-chemical properties with the antibacterial features of silver ions in a non-toxic form for the eukaryotic cells.

2. Materials and Methods

2.1 Materials. The sodium hyaluronate (*Phylcare Sodium Hyaluronate extra LW*) employed in this study was purchased from Biophil Italia Spa (MW ≈ 100 - 400 kDa). Sodium hyaluronate-

89 lipoate (SHL), prepared as previously reported, (Picotti et al., 2013) had a degree of substitution of
90 0.3 as determined by NMR analysis with a corresponding molar mass (MW) of the repeating unit
91 equal to 457.5 g mol^{-1}. Chemical identity of SHL was assessed by NMR, with reference to
92 published results.(Picotti et al., 2013). Hyaluronidase (type IV-S from bovine testes, H 3884 - 500
93 mg, batch 098K7352, 2140 units / mg, lyophilized powder) was purchased from Sigma Aldrich.
94 Neutral Red, Thiazolyl Blue Tetrazolium Bromide (MTT), phenazine methosulfate (PMS), bovine
95 serum albumin (BSA) powders, fetal bovine serum, Luria-Bertani (LB) broth, LB Agar, Brain Heart
96 Infusion (BHI) broth, silver acetate (≥ 99.0%) and phosphate buffered saline (PBS) were all
97 purchased from Sigma-Aldrich (Chemical Co. USA). Dulbecco's Modified Eagle's Medium, fetal
98 bovine serum, penicillin, streptomycin and glutamine solutions were purchased from EuroClone,
99 Italy. All chemicals and reagents were of the highest purity grade commercially available.

100 **2.2 Characterization methods.** NMR analyses were performed with a Bruker AVANCE 400
101 spectrometer, equipped with an indirect multinuclear gradient z probe (ID 5 mm BBI 1HBB z-
102 GRAD). UV-Vis measurements were performed on Varian Cary 50 spectrophotometer. Elemental
103 analysis was provided as a service by REDOX srl - Viale Stucchi, Monza -MB.

104 **2.3 Synthesis of SHLS12.** The synthesis of the silver complex of sodium hyaluronate-lipoate
105 (SHLS12) was performed simply by silver acetate addition (0.098 g; MW: 116.91 g mol^{-1}; 0.58
106 mmol, ratio with lipoic residue 1/1 mol/mol) to a 0.2% w/v solution of SHL (1 g anhydrous, 457.5 g
107 mol^{-1}, 2.18 mmol. in 0.5 L). A gel formation was observed after about two hours.

108 **2.4 Rheological measurements.** It has been used a control stress rheometer Anton Paar MCR
109 30, equipped with cone/plate (50 mm / 1°) and parallel plate (SPP 25 mm / gap 1 mm) measurement
110 systems. Studies were carried out on SHLS12 complex (0.2% w/v), sodium hyaluronate (0.2%
111 w/v), SHL (0.2% w/v), SHL after Ag removal and sodium hyaluronate (0.2% w/v) + silver. For the
112 latter it was added the same quantity of silver acetate used in SHLS12 synthesis, and the same
113 swelling time was considered. All solutions were prepared in acetate buffer 30 mM (pH = 5.4). All

samples were preliminarily characterized at 25 °C, while degradation studies were conducted at 37 °C for at least 2 hours, under continuous flow. Gelation kinetics was performed at 25 °C: silver acetate solution was added to 0.2% w/v of polymer solution (sodium hyaluronate or SHL) for each measurement. After 4 minutes under magnetic mixing, the samples were transferred on measurement system and test starts.

2.5 Enzymatic degradation. Enzymatic degradation studies were carried out with bovine testicular hyaluronidase: the molar ratio of polysaccharide / enzyme used was 6150:1 (referred to disaccharide unit of SHL). Degradation kinetic was conducted adding 70 µL of hyaluronidase concentrated solution to 1 mL of polymeric solutions or swelled complex, thermostated at 37 °C. The mixture was stirred for 30 seconds and then transferred to the measuring system. Rheological measurements started after 3 minutes from mixing.

2.6 Antibacterial tests. The antibacterial activity of SHLS12 was evaluated using strains of *Escherichia coli* (ATCC® 25922™), *Staphylococcus epidermidis* (ATCC® 12228™), *Staphylococcus aureus* (ATCC® 25923™) and *Pseudomonas aeruginosa* (ATCC® 27853™).

2.6.1 Growth inhibition assay. Growth inhibition assay was performed according to the protocol described in (Sacco, Travan, Borgogna, Paoletti, & Marsich, 2015) with slight modifications. SHLS12 solution (0.2% w/v) was prepared by adding SHLS12 in LB broth and vigorously vortexed for 30 seconds in order to obtain a clear and homogeneous dispersion of the polymer in such medium. Bacterial suspensions were prepared by adding 20 µL of bacteria, preserved in glycerol, to 5 mL of LB broth. The obtained suspensions were incubated overnight at 37 °C. After 24 h, 500 µL of bacterial suspension was diluted in 10 mL of broth and grown up for 90 min at 37 °C in order to restore an exponential growth phase. Bacterial concentration was measured by means of optical density (OD) at 600 nm. After centrifugation (3 500 rpm, 5 min), supernatants were removed and bacteria were resuspended with either SHLS12 solution in LB broth or LB broth to obtain a final concentration of 5×10^6 bacteria mL^{-1}. In the case of evaluation of the

BSA influence on SHLS12 activity, bacteria were resuspended in LB broth added with either BSA (40 g L^{-1}) or BSA and SHLS12 (40 g L^{-1} and 0.2% w/v, respectively). All bacteria strains were then incubated at 37 °C for 4 h in shaking conditions (140 rpm). At the end of incubation, bacterial suspension was serially diluted in PBS buffer (from 10^{-1} to 10^{-5}) and 25 µL of each suspension were plated on LB agar. After overnight incubation at 37 °C, the colony forming units (CFUs) were counted. Outcomes were compared with the suspension of bacteria grown in liquid medium as control.

2.6.2 Biofilm formation. Bacterial suspensions of *S. aureus* and *P. aeruginosa* were prepared by adding 20 µL of bacteria, preserved in glycerol, to 5 mL of BHI broth *plus* 3% w/v sucrose. The obtained suspensions were incubated overnight at 37 °C. After 24 h, bacteria were diluted 1:100 in the same broth and plated (300 µL/well) into 24-well plates. For confocal laser scanning microscopy analyses, bacteria were plated on sterile 13 mm tissue culture coverslips (Sarstedt, USA) laid down on the bottom of the culture plate wells. Plates were incubated at 37 °C for 24 h to allow biofilm formation. After 24 h, broth was removed and formed biofilm was carefully rinsed twice with 100 µL of sterile PBS in order to remove planktonic cells. 300 µL of PBS containing 0.2% w/v of SHLS12 were deposited on the bacterial layer. Biofilms were then incubated at 37 °C and MTT assay was performed according to the following protocol after 4 and 24 h of incubation.

2.6.3 Viable biomass assessment. The test was performed according to the protocol described elsewhere.(Brambilla et al., 2012) Briefly, MTT stock solution was prepared by dissolving 5 mg mL^{-1} of MTT powder in sterile PBS. PMS stock solution (0.3 mg mL^{-1}) was prepared by dissolving PMS powder in sterile PBS. Solutions were further filtered (0.22 µm filters, BioSigma, Italy) and stored at 2 °C in light-proof vials until the day of the experiment, when a fresh measurement solution (FMS) was prepared by mixing 0.5 mL of MTT stock solution, 0.5 mL of PMS stock solution, and 4 mL of sterile PBS. DMSO was used as lysing solution (LS). After the biofilm incubation period, SHLS12 and PBS were gently removed from the plates and each well was

carefully rinsed three times with 100 µL of sterile PBS in order to remove non-adherent cells. 200 µL of FMS solution were placed into each well and the plates were incubated for 3 h under light-proof conditions at 37 °C. The FMS solution was then gently removed and formazan crystals were dissolved by adding 200 µL of LS to each well. Plates were additionally stored for 1 h under light-proof conditions at room temperature and then 100 µL of the solution were transferred into the wells of 96-well plates. The absorbance of the solution was measured using a spectrophotometer (FLUOStar Omega-BMG Labtech) at a wavelength of 550 nm. Outcomes were expressed as OD units.

2.7 Confocal laser scanning microscopy (LSCM). LSCM analyses were addressed at detecting viability of bacteria in the biofilm mass. FilmTracer Live/Dead biofilm viability kit (Invitrogen™) was used. Dead cells were stained by propidium iodide (red fluorescence - λ_{ex} 514 nm; λ_{em} 590 nm), whereas living cells by SYTO® 9 (green fluorescence - λ_{ex} 488 nm; λ_{em} 515 nm). Staining was performed according to the manufacture's protocol on biofilms grown on coverslips as described above. Images were acquired on a Nikon Eclipse C1si confocal laser scanning microscope with a Nikon Plan Fluor 20X as objective. Stacks of images were analyzed using ImageJ software.

2.8 Cell culture. Mouse fibroblast-like NIH-3T3 (ATCC® CRL1658) and immortalized human keratinocyte HaCaT (kind gift of Dr. Chiara Florio, University of Trieste) cell lines were used for the *in vitro* experiments. Both cell lines were cultured in Dulbecco's Modified Eagle's Medium high glucose, 10% heat-inactivated fetal bovine serum, 100 U mL^{-1} penicillin, 100 µg mL^{-1} streptomycin and 2 mM L-glutamine in a humidified atmosphere of 5% CO_2 at 37 °C.

2.9 Biocompatibility studies. *In vitro* cytotoxicity of SHLS12 was evaluated by using Neutral Red assay on both NIH-3T3 and HaCaT cells. 20 000 cells were plated on 24-well plates and, after complete adhesion, culture medium was changed with 300 µL of fresh medium. The cytotoxicity test was performed by direct contact of the cells with SHLS12 (50 µL of a solution

189 0.2% w/v) laid down on filter papers, (16 mm^2 as surface) placed in the middle of each well. As a
190 positive control material, poly(urethane) films containing 0.25% zinc dibuthyldithiocarbamate
191 (ZDBC) were used. As negative control material, plastic poly(styrene) sheets were used. Untreated
192 cells (without any contact-material) were also considered as additional control. After 24 and 72 h,
193 Neutral Red assay was performed according to the manufacture's protocol. Each material test was
194 performed in triplicate. Cytotoxicity was expressed as percentage of viability by normalizing the
195 OD_{540} nm of treated cells to the OD_{540} nm of the untreated cells.

196 **2.10 Statistical analysis.** Data are expressed as means and standard deviations (SD).
197 Statistical analysis was performed using Student's t test, and a P value of < 0.05 was considered
198 statistically significant.

199 ## 3. Results and discussion

200 **3.1 SHLS12: physical-chemical properties.** The chemical characterization of the product
201 was initially carried out by NMR analysis, to reveal the interaction between SHL and silver ions. In
202 particular, the ^{1}H-NMR spectrum in D_2O of SHLS12 in comparison with SHL evidences signal
203 modifications at the lipoic ring level (Figure S2 of the Supplementary Material). More in detail, the
204 two protons in 6 position are down field shifted by presence of silver (H6a from 2.45 to 2.72 ppm,
205 H6b from 1.95 to 2.13 ppm) while the other protons, closer to the ester bond, are less affected. This
206 suggests that an interaction between the metal and the lipoic ring occurs. Moreover, a drift of the
207 anomeric signal is also observed, which is compatible with a conformational stiffening of the
208 polymer chain, as suggested by the signal broadening.

209 Assessing a possible role of the acetate moiety is of pivotal importance for the better
210 understanding of the structure of the complex. NMR can help evaluating whether the acetate ion is
211 somehow bound to the Ag^+-containing polymer system: upon increasing magnetic field strength the
212 signals of diffusive species decrease more rapidly than those of the groups bound to the polymer

(DOSY experiments). When the proton signals of the methyl group in acetate and in N-acetylglucosamine are compared with that of HDO (used as standard as diffusive species in solution), it was observed that the former decreases proportionally to that of HDO, while the intensity of that relative to N-acetylglucosamine is constant. It can be concluded that acetate is freely diffusible and not bound to the polymer domain (Figure S3 of the Supplementary Material).

The chemical and physical nature of silver in such biomaterial is crucial in relation to the biological activity of the complex. In order to determine whether silver was present as Ag^+ or in nanoparticle form, UV-Vis measurements were performed. Spectrum in Figure 1A shows that silver in SHLS12 is not in nanoparticle form because the typical plasmon resonance band at around 410 nm is absent. Moreover, by adding sodium iodide (NaI) as Ag^+-precipitating molecule, the gel structure is destroyed and a biphasic system is recovered, with a precipitate observed at the bottom. NMR analysis of the supernatant solution (Figure 1B) points out a pattern of signals perfectly matching those of native SHL, thus demonstrating the full reversibility of interaction with no permanent chemical modification. This evidence was also confirmed by rheological measurements (Figure 2B).

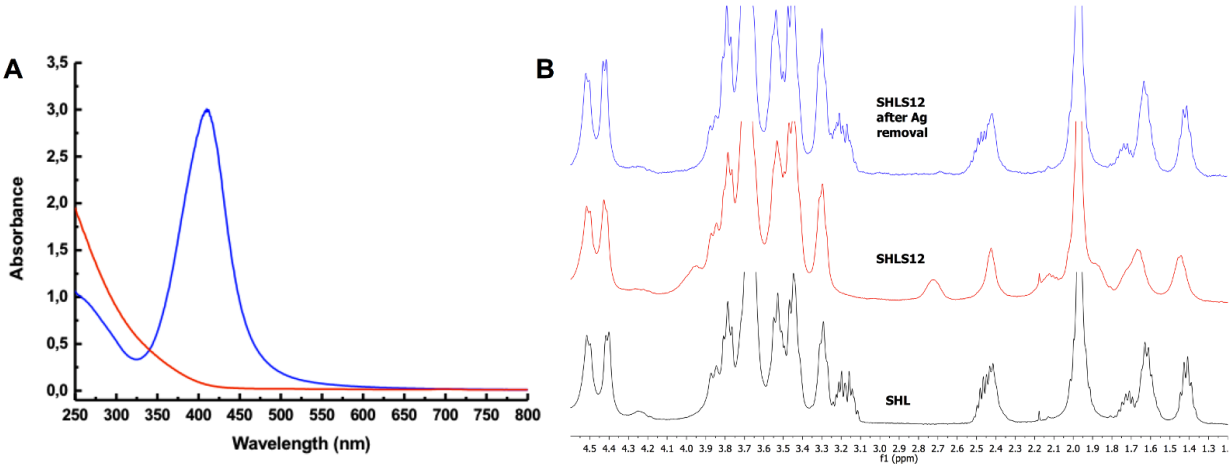

Figure 1. (A) UV-Vis spectra of SHLS12 compared to silver nanoparticles; (B) ^{1}H-NMR spectra of Sodium Hyaluronate-Lipoate (SHL), SHLS12 and SHLS12 after silver removal.

233 The ratio between the polymer and the metal was determined by means of conductometry.
234 SHL solution (10 mL; DS: 0.3 mol/mol; concentration 0.2% w/v ≈ 0.043 mM) was prepared and
235 silver acetate solution (45.2 mM) was drop wise added to it. Figure S4 reports the conductivity
236 values as a function of the volume of silver acetate solution added. The plot shows that the
237 conductivity trend undergoes a slope variation. By the linear fitting of experimental data, the point
238 of discontinuity was obtained corresponding to a ratio silver/lipoic residue of 1:1. Elemental
239 analysis (Theoretical: Silver: 6.9%; Sulphur: 4.1% - Found: Silver 6.6%; Sulphur 3.9%) on the
240 isolated product from precipitation with acetone confirmed the 1:1 ratio.

241 A rheological investigation was performed to point out differences among the various
242 systems. While sodium hyaluronate and its derivative SHL showed a solution-like behavior,
243 SHLS12 behaved like a gel. These results are highlighted in Figure 2A,B where the mechanical
244 spectra and flow curves are shown. A further control (sodium hyaluronate + silver) was added so as
245 to verify the role of metal with the polymer. We demonstrated that when silver was added to
246 sodium hyaluronate a solution-like behaviour was observed in both cases. In order to verify the gel
247 nature of SHLS12, a gelation kinetics was performed and the outcomes are shown in Figure 2C. We
248 observed the intersection between the storage and loss moduli about after 20 minutes of gelation.
249 Later, the storage modulus was verified to be almost one order of magnitude higher with respect to
250 the loss modulus. This condition allows considering SHLS12 as a “strong gel”. Conversely, a
251 solution-behavior was demonstrated when silver was added to sodium hyaluronate. Indeed, the loss
252 modulus was found constant on time. The straightforward explanation is that silver ions may act as
253 non-covalent linking points between sulphur atoms of the lipoic residues of the different chains
254 favoring the formation of a tridimensional network.

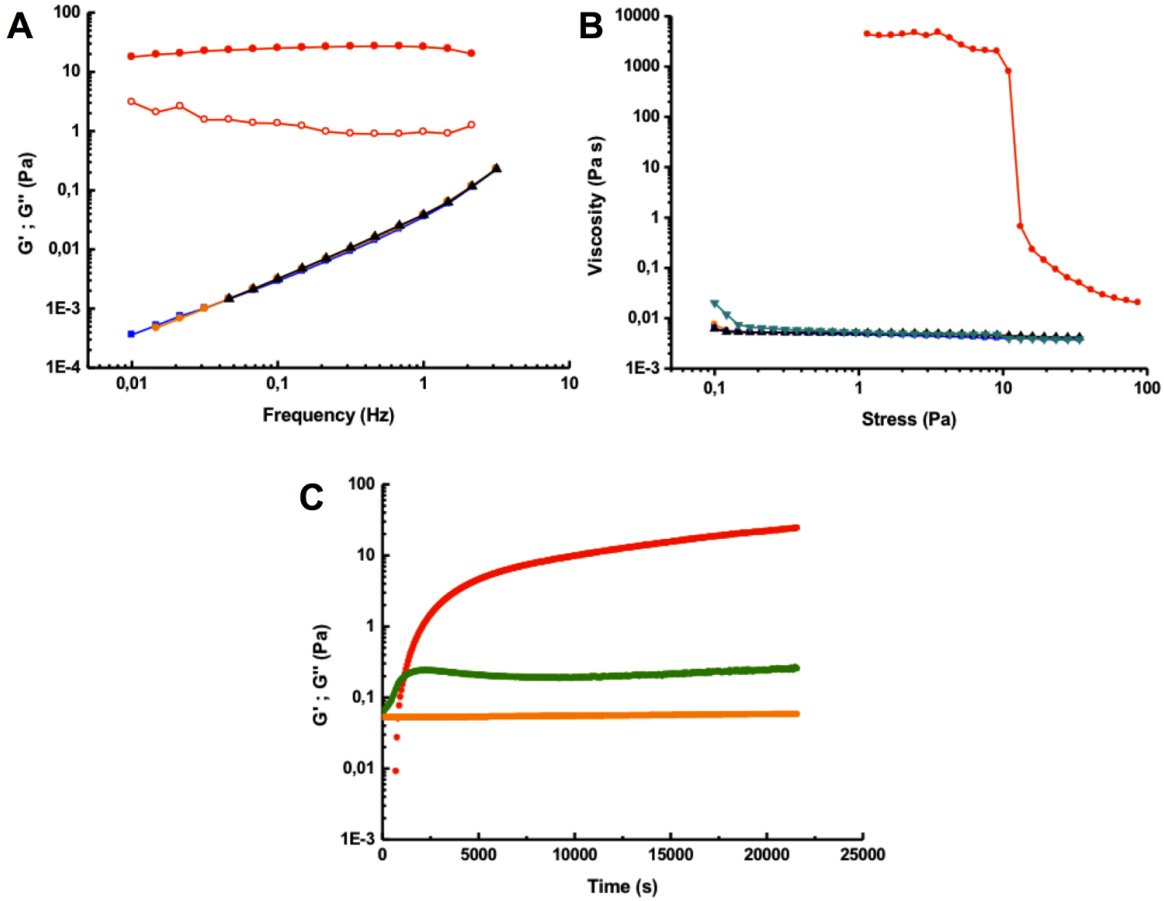

Figure 2. Mechanical spectra (A) of SHLS12 (red full - G' - and open - G" - circles), Sodium Hyaluronate-Lipoate (blue squares), Sodium Hyaluronate (black triangles) and Sodium Hyaluronate + silver (orange circles) loss moduli. Flow curves (B) of SHLS12 (red circles), Sodium Hyaluronate-Lipoate (blue squares), Sodium Hyaluronate (black triangles), Sodium Hyaluronate + silver (orange circles) and Sodium Hyaluronate-Lipoate after Ag removal (cyan triangles). Gelation kinetics (C): storage (red circles) and loss (green circles) moduli over time of SHLS12; Sodium Hyaluronate + silver (orange circles) loss modulus.

Enzymatic degradation tests were conducted to evaluate the complex resistance, in comparison with sodium hyaluronate and SHL: the results are shown in Figure 3. At the substrate/enzyme ratio tested, hyaluronan is quickly degraded: the viscosity value dropped to half in 10 minutes. After 20 minutes the degradation process was practically completed as seen by a reduction in viscosity of 70%. At the same substrate/enzyme ratio, SHL and SHL12 resisted enzymatic degradation for more than two hours. These results are pointed out in Figure 3A, where

degradation kinetics and their corresponding baseline (in the absence of enzyme) are plotted. Moreover, it was surprisingly found that SHLS12 maintained its gel nature, as shown in Figure 3B. Indeed, the storage modulus value was found to not vary over 2 hours at the substrate/enzyme ratio tested.

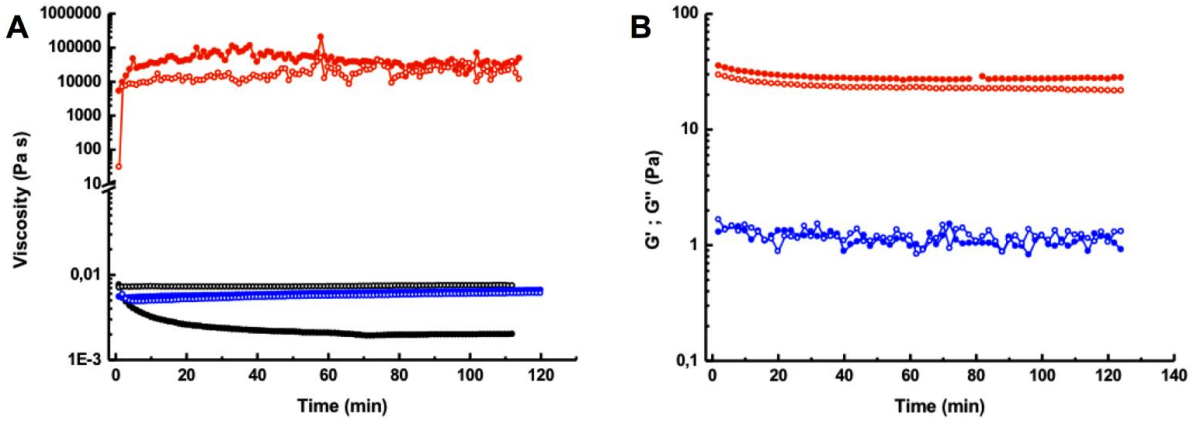

Figure 3. (A) Degradation kinetics (full symbols) and baselines (open symbols) reported as viscosity of SHLS12 (red circles), Sodium Hyaluronate-Lipoate (blue circles) and Sodium Hyaluronate (black circles). (B) Degradation kinetics (full symbols) and baselines (open symbols) reported as storage (red)/loss (blue) moduli of SHLS12 during hyaluronidase treatment. For all samples analysed the molar ratio of enzyme/substrate used was 1:6150.

3.2 Antibacterial properties. The pivotal feature of a silver-containing biomaterial concerns to its ability to exert antibacterial properties against different bacteria strains without impairing the viability of eukaryotic cells. In this study, we have explored the possibility by SHLS12 to affect the growth and viability of bacteria both in a planktonic and in an organized community state (biofilm). *E. coli*, *S. aureus*, *P. aeruginosa* and *S. epidermidis* strains were selected for this study because of their widespread diffusion and high probability to be engaged at an injury site in the human body and to favor the planktonic-sessile state transition. Figure 4 shows the results obtained by a growth inhibition assay. A small amount of SHLS12 (0.2% w/v) showed a marked antibacterial activity owing to the presence of silver ions whereas the formulation without silver (SHL) demonstrated lack of antibacterial properties (data not shown). For all strains investigated, a significant drop of

CFU (at least $P < 0.01$) was identified for SHLS12-treated samples in comparison with control (suspension of bacteria grown in broth). This finding is confirmed by visual observations as reported in Figure 4 E-H, which shows the growth of *S. aureus* colonies on LB agar for treated and untreated samples.

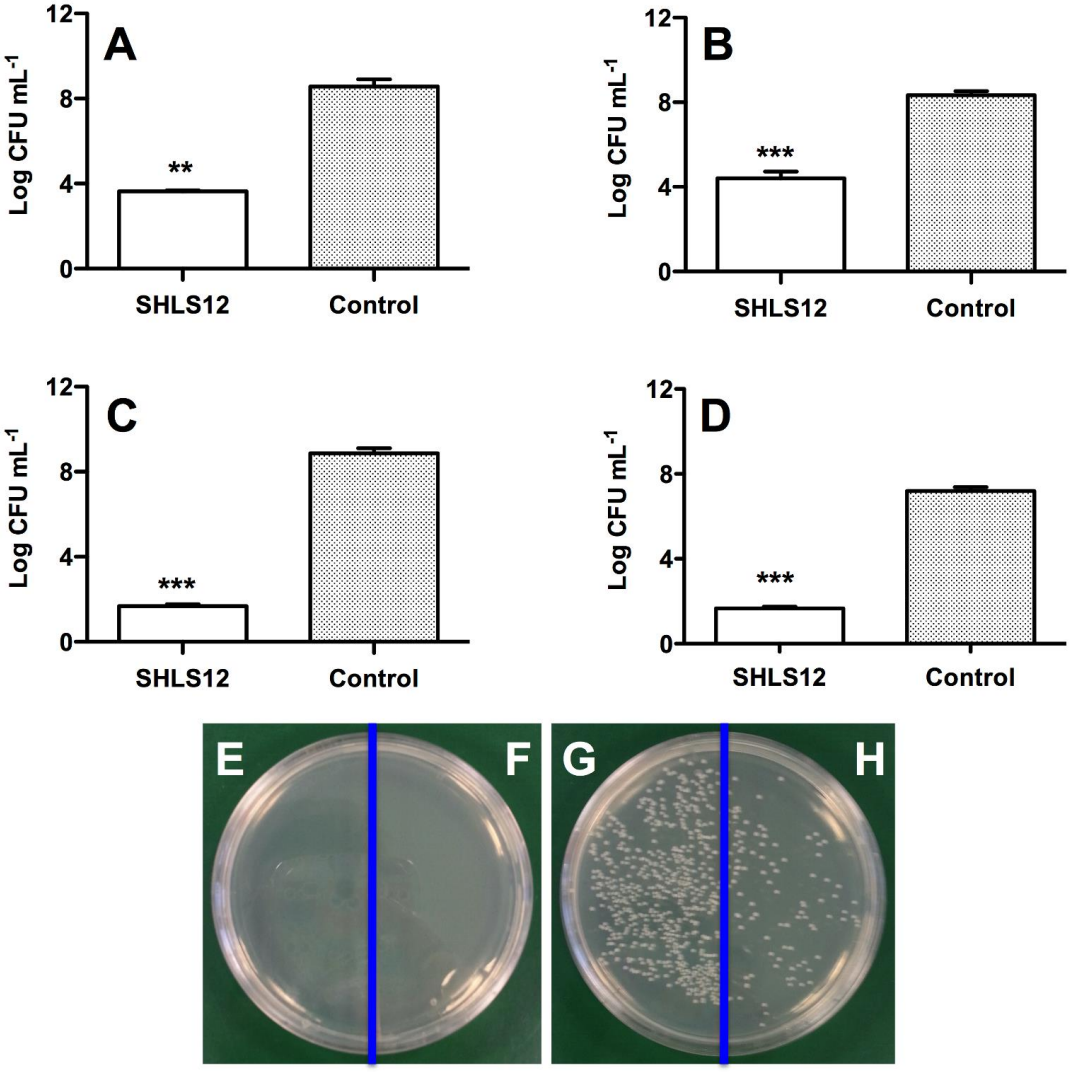

Figure 4. Growth inhibition rate expressed as Log CFU mL^{-1} of *S. aureus* (A), *S. epidermidis* (B), *E. coli* (C) and *P. aeruginosa* (D) following 4 h of treatment with SHLS12. Statistical differences were determined by means of Student's t test. $^{**}P < 0.01$; $^{***}P < 0.001$. *S. aureus* colonies on LB agar: diluted 10^{-4} (E) and diluted 10^{-5} (F) SHLS12-treated sample; diluted 10^{-4} (G) and diluted 10^{-5} (H) control sample.

Considering *in vivo* applications of SHLS12, the inactivation of silver by serum proteins can

be a concern. In particular, serum albumin has been shown to have specific binding sites for metal ions entering the bloodstream.(Deng, Wang, Zhu, Xu, & Ning, 2010),(Durgadas, Sharma, & Sreenivasan, 2011),(Duff & Kumar, 2009) They are best characterized for human serum albumin (HSA) and for bovine serum albumin (BSA), which is often used as a model protein for HSA.(Bal, Sokołowska, Kurowska, & Faller, 2013) Zhao *et al.* demonstrated the formation of complexes between Ag^+ and BSA by spectroscopic investigation.(Zhao, Liu, Teng, & Liu, 2011) Ostermeyer *et al.* demonstrated that BSA reduces the toxicity of citrate silver nanoparticles by chelating the silver ions released from silver nanoparticles (AgNPs) and by binding to AgNPs surface thus preventing NH_3-dependent dissolution from occurring.(Ostermeyer, Kostigen Mumuper, Semprini, & Radniecki, 2013) This phenomenon has also been investigated in a previous contribution by the authors of the here presented paper where the ability of serum proteins to reduce the antibacterial features of a colloidal solution of Chitlac-nAg was demonstrated.(E Marsich et al., 2013) It should be recalled that at physiological pH the overall charge of albumin is predominantly negative, and hence electrostatic interactions with the Chitlac polycation may be at the root of such an adverse effect. We selected BSA at a concentration of 40 g L^{-1} to verify its influence on the antibacterial properties of SHLS12. As shown in Figure 5, a significant drop of *S. aureus* and *P. aeruginosa* CFUs was demonstrated after 4 h of treatment with both SHLS12 and SHLS12 + BSA with respect to control. By comparing SHLS12 with SHLS12 + BSA treated samples, no statistical difference was identified for *S. aureus.* In the case of *P. aeruginosa* a significant but small difference was identified ($P < 0.05$), so as to evidence only a partial and minimal inhibitory effect of serum albumin towards SHLS12 antibacterial activity. At variance with the case of Chitlac, a favorable electrostatic contribution by the anionic nature of the hyaluronan backbone to prevent association with albumin can be reasonably postulated for SHLS12.

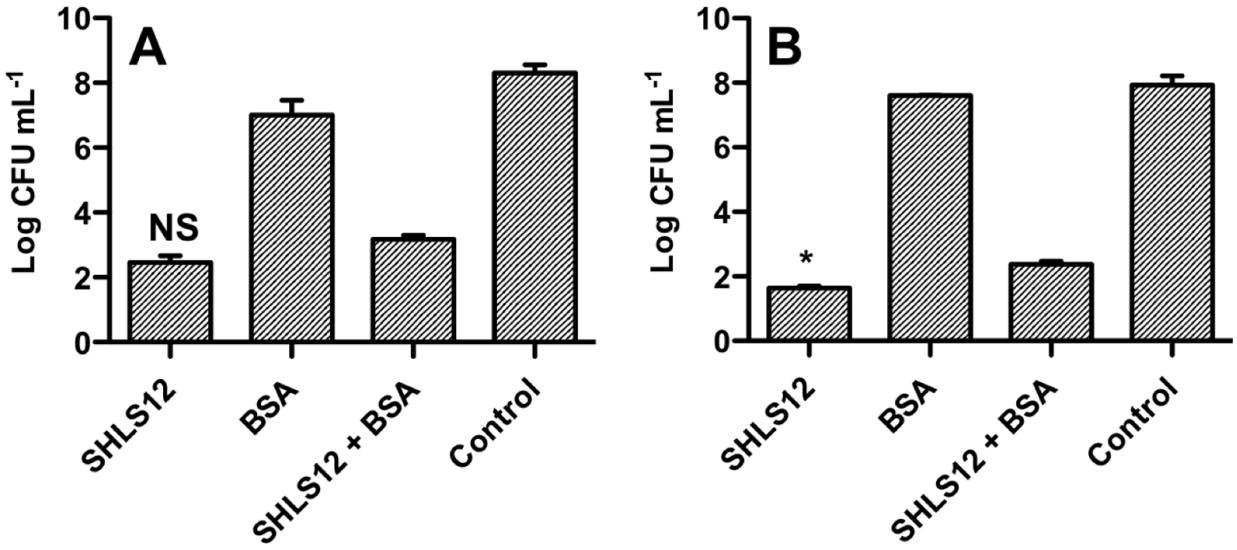

330 **Figure 5.** Growth inhibition rate in the presence/absence of BSA expressed as Log CFU mL^{-1} of *S.*
331 *aureus* (A) and *P. aeruginosa* (B) following 4 h of treatment with SHLS12. Statistical differences
332 were determined by means of Student's t test. NS no statistical differences between SHLS12 and
333 SHLS12 + BSA-treated samples; $*P < 0.05$ between SHLS12 and SHLS12 + BSA-treated samples.
334

335 Another key issue that has been considered in the present work is the capability of the silver-
336 complex to exert antibacterial activity towards organized-community of bacteria, so called biofilms.
337 In such condition, an extracellular polymeric substance (EPS) surrounds the bacterial cells making
338 them one thousand times more resistant to antibiotics and drugs than planktonic ones.(Pelgrift &
339 Friedman, 2013) *S. aureus* and *P. aeruginosa* were selected for these studies because of their ability
340 to form biofilms.(Sacco et al., 2015),(Hindi et al., 2009) Figure 6 A-B summarizes the outcomes
341 obtained after 4 and 24 h of treatment of *S. aureus* and *P. aeruginosa* biofilms, respectively. In both
342 cases, SHLS12 was effective in breaking apart the biofilm, as revealed by MTT colorimetric assay.
343 The optical density (OD) of *S. aureus* treated with SHLS12 showed a reduction of about 30% after
344 24 h of treatment with respect to the control, whereas no statistical difference was observed after 4
345 h of treatment. As contrast, in the case of *P. aeruginosa*, a marked OD reduction was evident
346 already after 4 h of treatment. It may be argued that *P. aeruginosa* is more susceptible than *S.*
347 *aureus* strain to Ag^{+} ions, likely because of their thinner cell wall, which enables silver ions to
348 penetrate into the bacterial cell more easily.(Huang, Dai, Xuan, Tegos, & Hamblin, 2011) These

results were confirmed by differential biofilm staining for dead (red) and alive (green) cells and visualization with confocal laser scanning microscopy after treatment with SHLS12. In Figure 6 C-F *P. aeruginosa* and *S. aureus* biofilms appear as a green fluorescent layer indicating the good bacteria viability in the case of the control. On the contrary, samples of cells treated for 24 h with SHLS12 evidenced the presence of a non-homogeneous layer of bacteria with few viable green cells and a lot of reddish/yellow bacteria, thus suggesting cell suffering and biofilm disaggregation. These findings are in agreement with what evidenced in the viable biomass experiments reported above. Overall, growth inhibition assays and viable biomass assessment clearly proved antibacterial properties of SHLS12 thanks to the presence of silver ions which, as reported in literature, exert their activity (*i*) by interacting with thiol/phosphorus-groups of the cell wall and the plasma membrane proteins of bacteria,(Pelgrift & Friedman, 2013),(Travan et al., 2011) causing membrane damage or (*ii*) by binding DNA of microbes leading to cell division alterations.(Hindi et al., 2009)

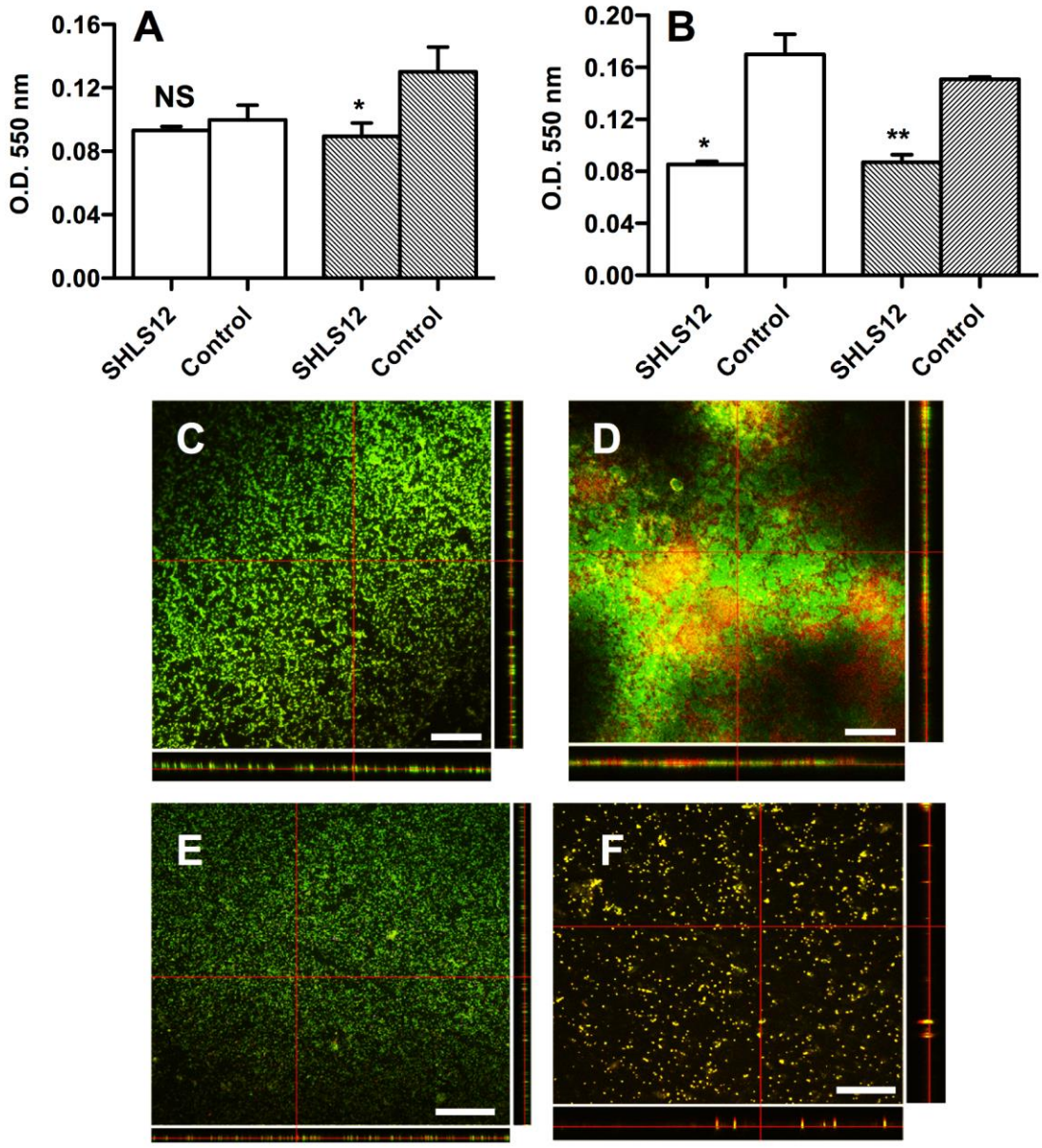

364
365

366 **Figure 6.** Viable biomass MTT assay expressed as O.D. at 550 nm of *S. aureus* (A) and *P.*
367 *aeruginosa* (B) following 4 (empty columns) and 24 h (filled columns) of treatment with SHLS12.
368 Statistical differences were determined by means of Student's t test. NS no statistical differences
369 versus control; **P* < 0.05 versus control; ***P* < 0.01 versus control. LSCM images of *P. aeruginosa*
370 biofilm: control group (C) and SHLS12-treated sample (D). LSCM images of *S. aureus* biofilm:
371 control group (E) and SHLS12-treated sample (F). Biofilms were grown on tissue culture coverslips
372 in BHI broth *plus* 3% w/v sucrose and following treated with SHLS12 for 24 hours. For cell
373 staining, FilmTracer Live/Dead biofilm viability kit (Invitrogen™) was used. Green fluorescence
374 indicates live cells whereas red and yellow fluorescence refers to dead and suffering ones,
375 respectively. Scale bar was 50 µm for all images.

3.3 Biocompatibility studies. One of the most important challenges in the production of silver-containing biomaterials concerns their ability to exert antibacterial activity without impairing the viability of eukaryotic cells. The toxicity of silver for eukaryotic cells is proportional to the amount of metal present in cell-containing environment, since it is able to cause cellular damages if the cells can uptake and internalize the metal.(Y.-H. Lee et al., 2014) A key strategy to reduce silver toxicity resides then in the development of systems capable to avoid - or at least reduce - the release of silver in a form available to eukaryotic cell uptake, but at the same time, preserve its antimicrobial activity allowing for the direct interaction of the metal ions with the proteins localized on the bacterial surface.

Polysaccharide-based matrices loaded with silver nanoparticles have been already described to prevent an excess of silver release and thus not to affect the viability of mammalian cells.(Sacco et al., 2015),(Travan et al., 2009),(Eleonora Marsich et al., 2013) In this view, it is plausible that the amount of released metal in these systems is under the lethal dose limit and thus not cytotoxic. In order to assess the biocompatibility of SHLS12, a Neutral Red cytotoxicity assay was carried out. It is based on the ability of viable cells to incorporate and bind the Neutral Red Supravital dye into the lysosomes.(Repetto, del Peso, & Zurita, 2008) Viable cells take up the dye by active transport whereas non-viable cells do not. Keratinocytes (HaCaT) and fibroblasts (NIH-3T3) cell lines were selected because of their broad use as models to evaluate the response of biological systems towards biopolymer networks.(Barui, Khare, Dhara, Banerjee, & Chatterjee, 2014) As reported in Figure 7, SHLS12 did not exert any cytotoxic effect on the cell lines used. In fact, there was no significant difference in Neutral Red signal between the SHLS12-treated and untreated cells after 24 and 72 h. The results of the positive control group on NIH-3T3 cells showed an apparently inexplicable result, namely a similar percentage of viability as the negative control after 4 h of treatment. However, this is likely ascribed to the slow developing cytotoxic activity of zinc dibuthyldithiocarbamate in poly(urethane) films towards such cell line. In spite of this, cells

appeared to be suffering by optical microscopy analyses: changes in morphology and appearance of suffering signals as well as chromatin aggregation (data not shown). At 72 h the cytotoxicity of the positive control was clear in all cases. The combination of the results shows that SHLS12, besides providing a good antibacterial activity against biofilm-forming bacteria strains, is not harmful to mammalian cells likely because its silver ions are firmly coordinated and immobilized by the lipoate groups and therefore do not diffuse into the surrounding environment.

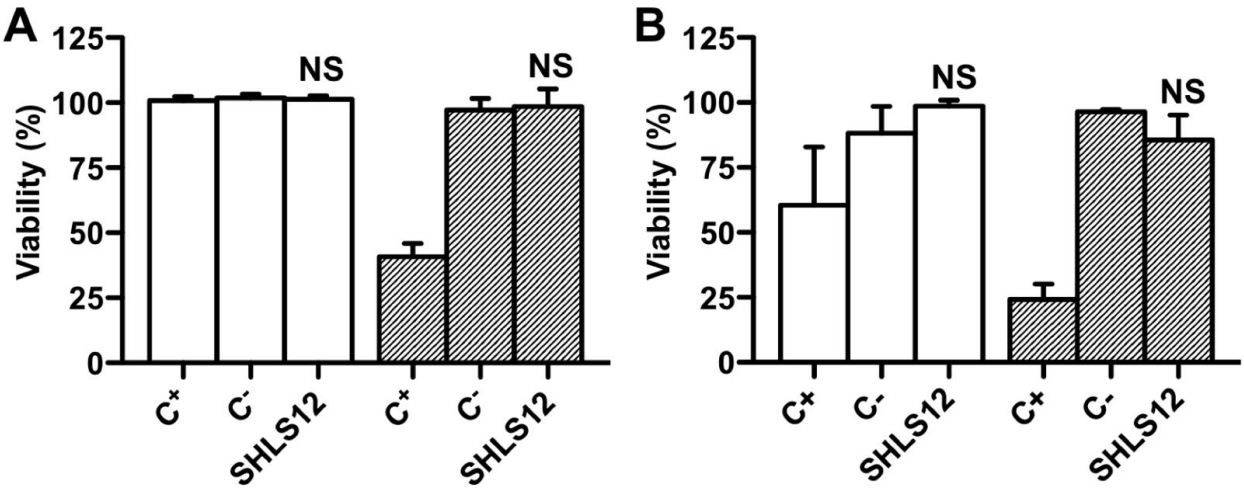

Figure 7. Percentage of viability of fibroblast NIH-3T3 (A) and ketatinocytes HaCaT (B) cells measured using Neutral Red assay. SHLS12 was kept in touch with cells and testing was performed after 24 (empty columns) and 72 h (filled columns) of treatment. Poly(urethane) sheets containing 0.25% zinc dibuthyldithiocarbamate were used as contact positive control (C^+) whereas plastic poly(styrene) sheets were used as contact negative control (C^-). Statistical differences were determined by means of Student's t test.

4. Conclusions

According to the chemical-physical studies, SHLS12 shows a strong viscoelastic behavior, in contrast to its polysaccharide precursor, thus suggesting the formation of a network with silver ions as linking points between the sulphur atoms of the lipoic residues. The overall result is a gel which is resistant to enzymatic degradation. This property should confer to the material an improved

biological stability *in vivo*. Such features, together with the demonstrated antibacterial properties and lack of cytotoxicity towards eukaryotic cells, allow considering SHLS12 a promising bioactive system for further *in vivo* applications.

Acknowledgements

This study was supported by the Friuli-Venezia Giulia Regional Government (Project: "Nuovi biomateriali per terapie innovative nel trattamento delle ferite difficili"-LR 47/78). The financial support to P.S. (PhD scholarship) by the Friuli-Venezia Giulia Regional Government and by the European Social Fund (S.H.A.R.M. project-Supporting human assets in research and mobility) is gratefully acknowledged.

References

Abdel-Mohsen, A. M., Hrdina, R., Burgert, L., Krylová, G., Abdel-Rahman, R. M., Krejčová, A., et al. (2012). Green synthesis of hyaluronan fibers with silver nanoparticles. *Carbohydrate Polymers*, *89*(2), 411–22.

Bal, W., Sokołowska, M., Kurowska, E., & Faller, P. (2013). Binding of transition metal ions to albumin: sites, affinities and rates. *Biochimica et Biophysica Acta*, *1830*(12), 5444–55.

Barui, A., Khare, R., Dhara, S., Banerjee, P., & Chatterjee, J. (2014). Ex vivo bio-compatibility of honey-alginate fibrous matrix for HaCaT and 3T3 with prime molecular expressions. *Journal of Materials Science. Materials in Medicine*, *25*(12), 2659–67.

Brambilla, E., Ionescu, A., Gagliani, M., Cochis, A., Arciola, C. R., & Rimondini, L. (2012). Biofilm formation on composite resins for dental restorations: an in situ study on the effect of chlorhexidine mouthrinses. *The International Journal of Artificial Organs*, *35*(10), 792–9.

Bustamante, J. (1998). α-Lipoic Acid in Liver Metabolism and Disease. *Free Radical Biology and Medicine*, *24*(6), 1023–1039.

Chudobova, D., Nejdl, L., Gumulec, J., Krystofova, O., Rodrigo, M. A. M., Kynicky, J., et al. (2013). Complexes of Silver(I) Ions and Silver Phosphate Nanoparticles with Hyaluronic Acid and/or Chitosan as Promising Antimicrobial Agents for Vascular Grafts. *International Journal of Molecular Sciences*, *14*(7), 13592–614.

Collins, M. N., & Birkinshaw, C. (2013). Hyaluronic acid based scaffolds for tissue engineering--a review. *Carbohydrate Polymers*, *92*(2), 1262–79.

Deng, B., Wang, Y., Zhu, P., Xu, X., & Ning, X. (2010). Study of the binding equilibrium between Zn(II) and HSA by capillary electrophoresis-inductively coupled plasma optical emission spectrometry. *Analytica Chimica Acta*, *683*(1), 58–62.

Duff, M. R., & Kumar, C. V. (2009). The metallomics approach: use of Fe(II) and Cu(II) footprinting to examine metal binding sites on serum albumins. *Metallomics : Integrated Biometal Science*, *1*(6), 518–23.

Durgadas, C. V, Sharma, C. P., & Sreenivasan, K. (2011). Fluorescent gold clusters as nanosensors for copper ions in live cells. *The Analyst*, *136*(5), 933–40.

Gunasekaran, T., Nigusse, T., & Dhanaraju, M. D. (2011). Silver nanoparticles as real topical bullets for wound healing. *The Journal of the American College of Clinical Wound Specialists*, *3*(4), 82–96.

Hindi, K. M., Ditto, A. J., Panzner, M. J., Medvetz, D. A., Han, D. S., Hovis, C. E., et al. (2009). The antimicrobial efficacy of sustained release silver-carbene complex-loaded L-tyrosine polyphosphate nanoparticles: characterization, in vitro and in vivo studies. *Biomaterials*, *30*(22), 3771–9.

Huang, L., Dai, T., Xuan, Y., Tegos, G. P., & Hamblin, M. R. (2011). Synergistic combination of chitosan acetate with nanoparticle silver as a topical antimicrobial: efficacy against bacterial burn infections. *Antimicrobial Agents and Chemotherapy*, *55*(7), 3432–8.

Kagan, V. E., Shvedova, A., Serbinova, E., Khan, S., Swanson, C., Powell, R., & Packer, L. (1992). Dihydrolipoic acid—a universal antioxidant both in the membrane and in the aqueous phase. *Biochemical Pharmacology*, *44*(8), 1637–1649.

Klasen, H. . (2000). A historical review of the use of silver in the treatment of burns. II. Renewed interest for silver. *Burns*, *26*(2), 131–138.

Knetsch, M. L. W., & Koole, L. H. (2011). New Strategies in the Development of Antimicrobial Coatings: The Example of Increasing Usage of Silver and Silver Nanoparticles. *Polymers*, *3*(4), 340–366.

Lee, S. J., Heo, D. N., Moon, J.-H., Ko, W.-K., Lee, J. B., Bae, M. S., et al. (2014). Electrospun chitosan nanofibers with controlled levels of silver nanoparticles. Preparation, characterization and antibacterial activity. *Carbohydrate Polymers*, *111*, 530–7.

Lee, Y.-H., Cheng, F.-Y., Chiu, H.-W., Tsai, J.-C., Fang, C.-Y., Chen, C.-W., & Wang, Y.-J. (2014). Cytotoxicity, oxidative stress, apoptosis and the autophagic effects of silver nanoparticles in mouse embryonic fibroblasts. *Biomaterials*, *35*(16), 4706–15.

Marsich, E., Bellomo, F., Turco, G., Travan, A., Donati, I., & Paoletti, S. (2013). Nano-composite scaffolds for bone tissue engineering containing silver nanoparticles: preparation, characterization and biological properties. *Journal of Materials Science. Materials in Medicine*, *24*(7), 1799–807.

Marsich, E., Travan, A., Donati, I., Turco, G., Kulkova, J., Moritz, N., et al. (2013). Biological responses of silver-coated thermosets: an in vitro and in vivo study. *Acta Biomaterialia*, *9*(2), 5088–99.

489 Ostermeyer, A.-K., Kostigen Mumuper, C., Semprini, L., & Radniecki, T. (2013). Influence of
490 bovine serum albumin and alginate on silver nanoparticle dissolution and toxicity to
491 Nitrosomonas europaea. *Environmental Science & Technology*, *47*(24), 14403–10.

492 Pelgrift, R. Y., & Friedman, A. J. (2013). Nanotechnology as a therapeutic tool to combat microbial
493 resistance. *Advanced Drug Delivery Reviews*, *65*(13-14), 1803–15.

494 Picotti, F., Fabbian, M., Gianni, R., Sechi, A., Stucchi, L., & Bosco, M. (2013). Hyaluronic acid
495 lipoate: synthesis and physicochemical properties. *Carbohydrate Polymers*, *93*(1), 273–8.

496 Ramachandran, L., & Krishnan Krishnan Nai, C. (2011). Therapeutic Potentials of Silver
497 Nanoparticle Complex of α-Lipoic Acid. *Nanomaterials and Nanotechnology*, *1*(2), 17–24.

498 Repetto, G., del Peso, A., & Zurita, J. L. (2008). Neutral red uptake assay for the estimation of cell
499 viability/cytotoxicity. *Nature Protocols*, *3*(7), 1125–31.

500 Sacco, P., Travan, A., Borgogna, M., Paoletti, S., & Marsich, E. (2015). Silver-containing
501 antimicrobial membrane based on chitosan-TPP hydrogel for the treatment of wounds. *Journal*
502 *of Materials Science: Materials in Medicine*, *26*(3), 128.

503 Travan, A., Marsich, E., Donati, I., Benincasa, M., Giazzon, M., Felisari, L., & Paoletti, S. (2011).
504 Silver-polysaccharide nanocomposite antimicrobial coatings for methacrylic thermosets. *Acta*
505 *Biomaterialia*, *7*(1), 337–46.

506 Travan, A., Pelillo, C., Donati, I., Marsich, E., Benincasa, M., Scarpa, T., et al. (2009). Non-
507 cytotoxic silver nanoparticle-polysaccharide nanocomposites with antimicrobial activity.
508 *Biomacromolecules*, *10*(6), 1429–35.

509 Xiu, Z., Zhang, Q., Puppala, H. L., Colvin, V. L., & Alvarez, P. J. J. (2012). Negligible particle-
510 specific antibacterial activity of silver nanoparticles. *Nano Letters*, *12*(8), 4271–5.

511 Yang, J., Zheng, H., Han, S., Jiang, Z., & Chen, X. (2015). The synthesis of nano-silver/sodium
512 alginate composites and their antibacterial properties. *RSC Adv.*, *5*(4), 2378–2382.

513 Zhao, X., Liu, R., Teng, Y., & Liu, X. (2011). The interaction between Ag+ and bovine serum
514 albumin: a spectroscopic investigation. *The Science of the Total Environment*, *409*(5), 892–7.

515